Science Advances
AAAS

advances.sciencemag.org/cgi/content/full/7/3/eabc4897/DC1

Supplementary Materials for

Multiple screening approaches reveal HDAC6 as a novel regulator of glycolytic metabolism in triple-negative breast cancer

Catríona M. Dowling, Kate E. R. Hollinshead, Alessandra Di Grande, Justin Pritchard, Hua Zhang, Eugene T. Dillon, Kathryn Haley, Eleni Papadopoulos, Anita K. Mehta, Rachel Bleach, Andreas U. Lindner, Brian Mooney, Heiko Düssmann, Darran O'Connor, Jochen H. M. Prehn, Kieran Wynne, Michael Hemann, James E. Bradner, Alec C. Kimmelman, Jennifer L. Guerriero, Gerard Cagney, Kwok-Kin Wong, Anthony G. Letai, Tríona Ní Chonghaile*

*Corresponding author. Email: tnichonghaile@rcsi.ie

Published 15 January 2021, *Sci. Adv.* **7**, eabc4897 (2021)
DOI: 10.1126/sciadv.abc4897

The PDF file includes:

Other Supplementary Material for this manuscript includes the following:

(available at advances.sciencemag.org/cgi/content/full/7/3/eabc4897/DC1)

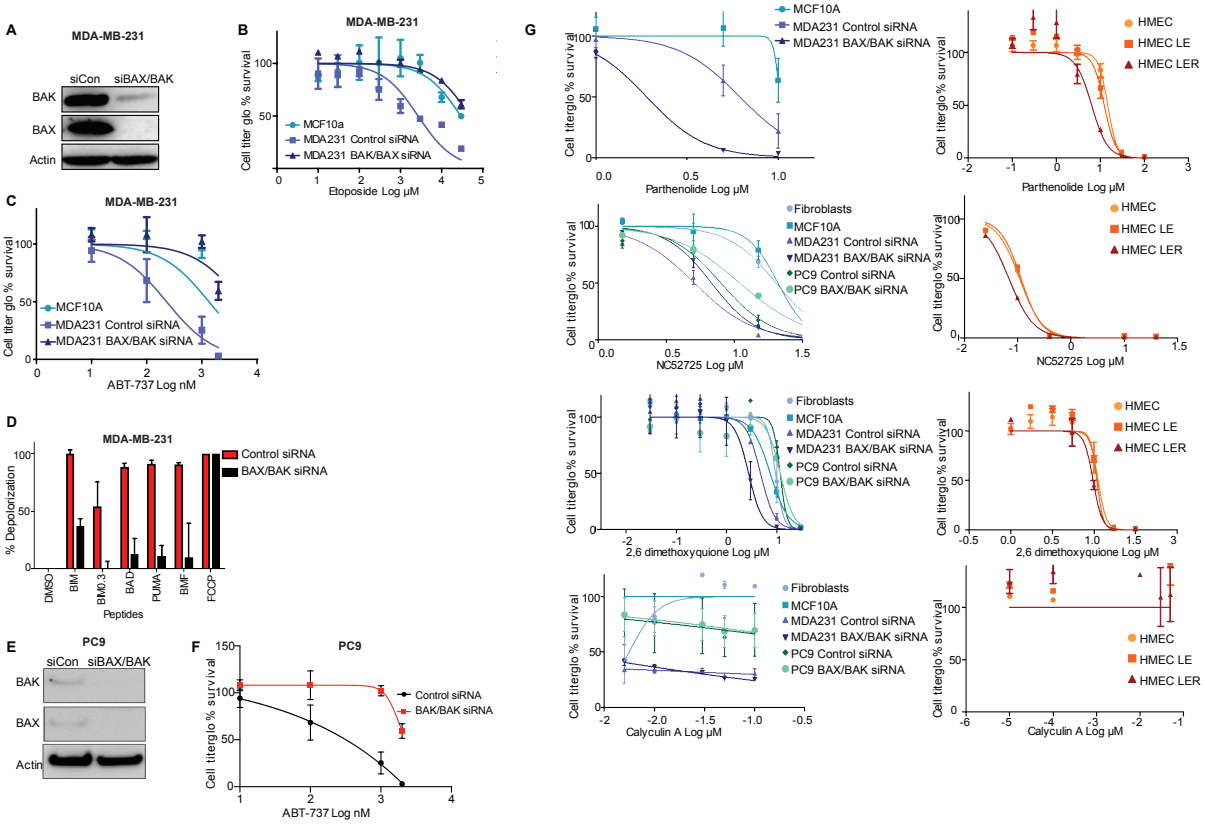

Fig. S1. Validation of lead hits from screen. (**A**) Representative Western blot showing knockdown of BAK and BAX in MDA231 cells with actin as loading control. (**B**) Response of MCF10a and MDA231 cells transfected with control or BAX and BAK to etoposide or (**C**) ABT-737 following 48 hr treatment (n=3, mean ± SD). (**D**) BH3 profiling examining the response of MDA231 cells to BH3 peptides following control or BAX/BAK knockdown (n=3, mean ± SD). (**E**) Western of BAK and BAX knockdown in PC9 cells transfected with control or BAX/BAK siRNA, with actin as loading control. (**F**) Response of PC9 cells control or BAX and BAK KD to ABT-737 (n=3, mean± SD) (**G**) Cell viability of cell lines treatment with indicated compounds for 48 hrs. Data graphed is mean ± SEM of three independent experiments.

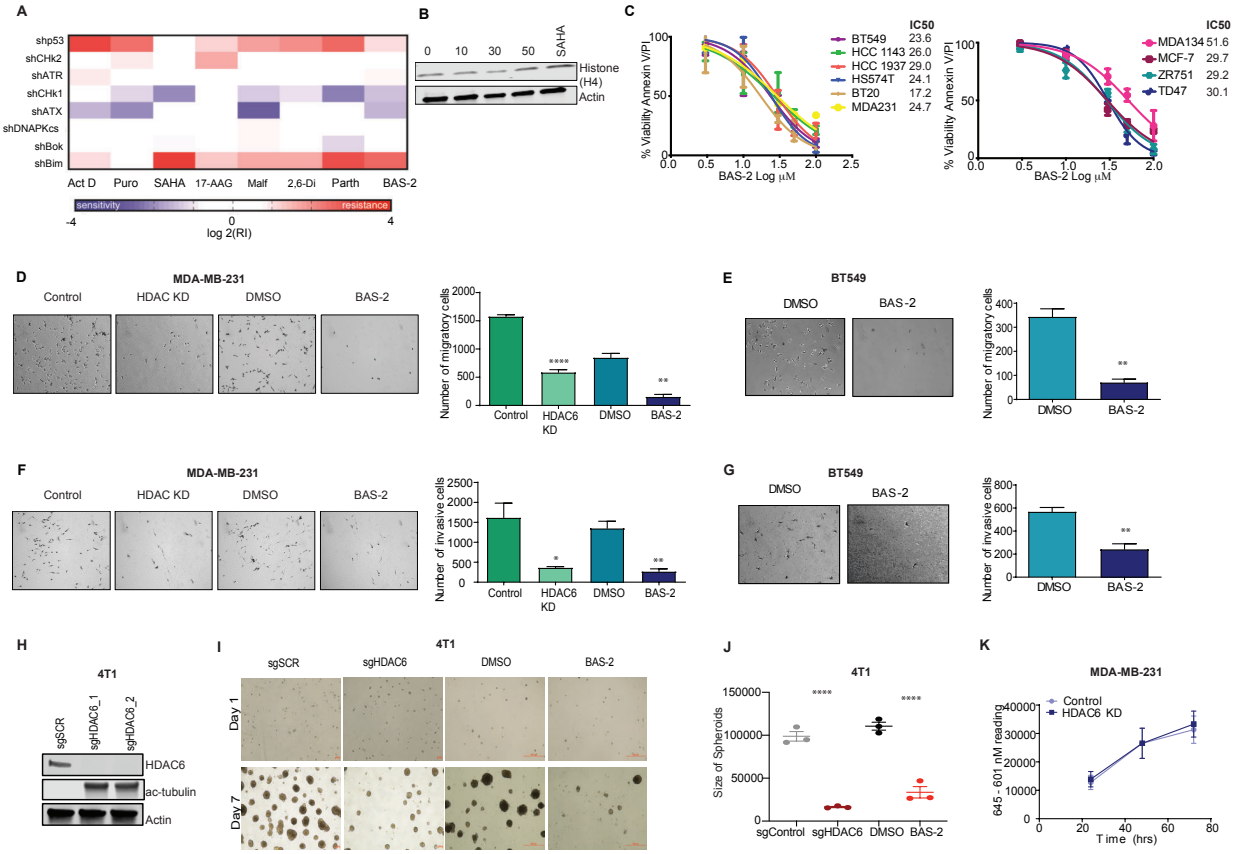

Fig. S2. BAS-2 induces the same phenotypical changed as HDAC6 knockdown in TNBC. (**A**) A heat map showing the response of cells expressing the indicated shRNAs to known compounds. Log-transformed RI values are shown. (**B**) Western blot demonstrating the acetylation of histone-4 in the presence of BAS-2 and SAHA with actin as loading control. (**C**) A dose-response of a panel of triple negative breast cancer and ER^+ breast cancer cell lines treated with BAS-2 for 48 hrs (n = 3, mean ± SEM). (**D**) Images of a migration assay of MDA231 cells following 24 hrs treatment. The bar graph represents the number of migratory cells (n=3, mean ± SD). (**E**) Images of a migration assay of BT-549 cells following 24 hrs treatment. Migratory cell numbers are graphed (n=3, mean ± SD). (**F**) Images of an invasion assay of MDA231 cells following 48 hrs. The number of invasive cells is graphed (n=3, mean ± SD). (**G**) Images of an invasion assay of BT-549 cells following 48 hrs treatment. The number of invasive cells is graphed (n=3, mean ± SD). (**H**) Western blot showing HDAC6 levels and acetylated tubulin in HDAC6 KO and control 4T1 cells, with actin as a loading control. (**I**) Images of 4T1 cells grown in matrigel for 7 days with HDAC6 KO or following treatment with 30 μM BAS-2. (**J**) Dot plots show the size of colonies in all treatment groups (n=3, mean ± SD). (**K**) Proliferation of MDA231 cells stably expressing a shRNA against HDAC6 (HDAC6 KD) or a scramble shRNA (Control).

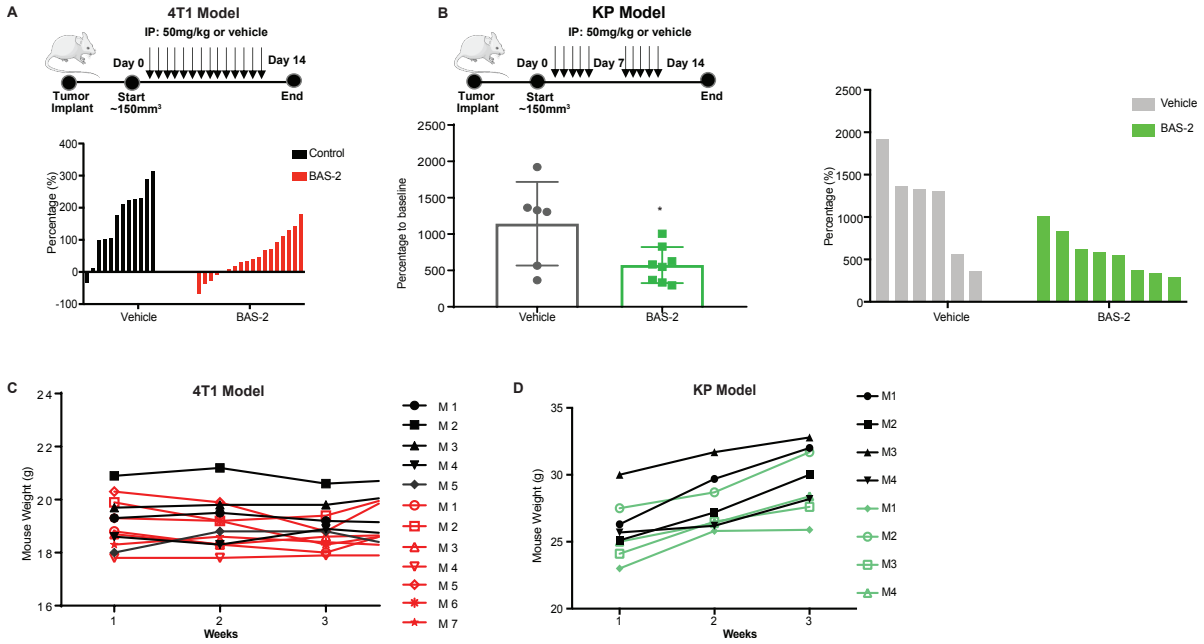

Fig. S3. BAS-2 reduces tumor volume in different cancer models. (**A**) BALB/cJ mice were subcutaneously inoculated with 4T1 ($0.1x10^6$) cells and treated with 50 mg/kg BAS-2 for 14 days. Waterfall plot illustrating response to BAS-2 treatment after 8 days of treatment. Each column represents one mouse, compared to baseline tumor measurement. (**B**) C57BL/6 mice were subcutaneously inoculated with KP ($0.5x10^6$) cells and following tumor formation mice were treated with vehicle or 50 mg/kg BAS-2. The mice were culled at the end of the experiment day 14. Tumors were measured and plotted as percentage change in tumor size following treatment (mean ± SEM, n=3, *P-value<0.05, unpaired student T-test). Waterfall plot illustrating response to BAS-2 treatment after 14 days of treatment. Each column represents one mouse, compared to baseline tumor measurement. (**C**) Weight of mice from 4T1 model taken each week. (**D**) Weight of mice from KP model taken each week.

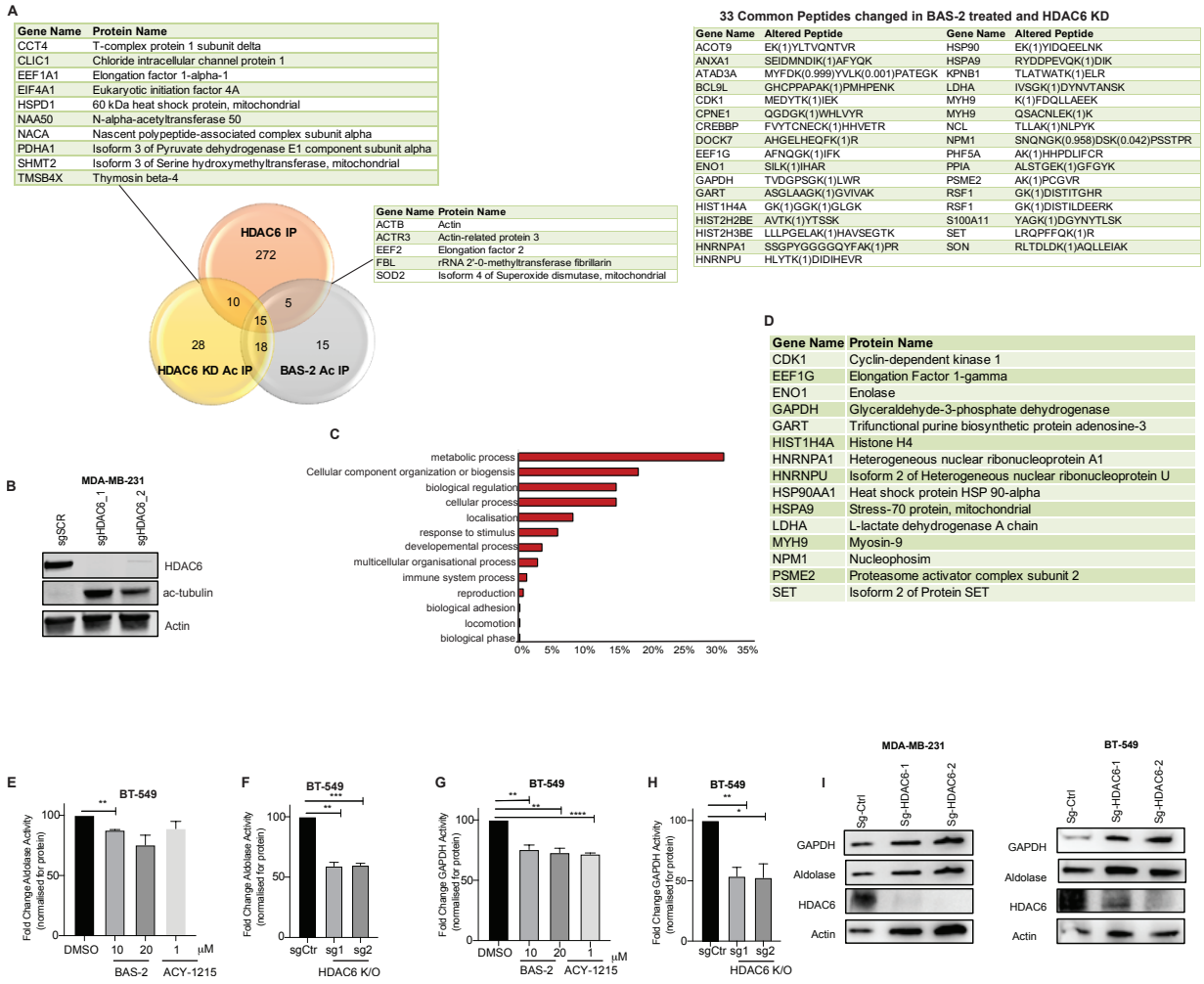

Fig. S4. Overlap of acetylated peptides and HDAC6 interactions. (**A**) Overlap of proteins identified between the significantly enriched proteins of the HDAC6 immunoprecipitation and enriched acetylated peptides from BAS-2 and HDAC6 experiments. Tables show names of proteins that are common between groups, in particular the 33 overlapping peptides between BAS-2 treated and HDAC6 KD. The figure in brackets refers to the modification localization score (acetylation) calculated by Maxquant program. (**B**) Western blot demonstrating HDAC6 level and acetylated tubulin in HDAC6 KO and control MDA231 cells, with actin as loading control (**C**) Bar graph showing the biological pathways altered by HDAC6 interacting proteins, as assessed by Panther. (**D**) List of 15 proteins which were identified in the LC-MS/MS acetylome and interactome experiments. (**E**) Measurement of aldolase enzymatic activity in BT-549 cell lysates following 24 hr BAS-2 treatment or ACY-1215 treatment. Activities were normalized to the total protein amount. (**F**) Same as (**E**) for HDAC6 KO. (**G**) Measurement of GAPDH enzymatic activity in BT-549 cell lysates following 24 hr BAS-2 treatment or ACY-1215 treatment. Activities were normalized to total protein. (**H**) Same as (G) for HDAC6 KO. (**I**) Western blots demonstrating the expression of Aldolase and GAPDH in MDA231 and BT-549 cells following HDAC6 KO. (n=3, mean ± SEM).

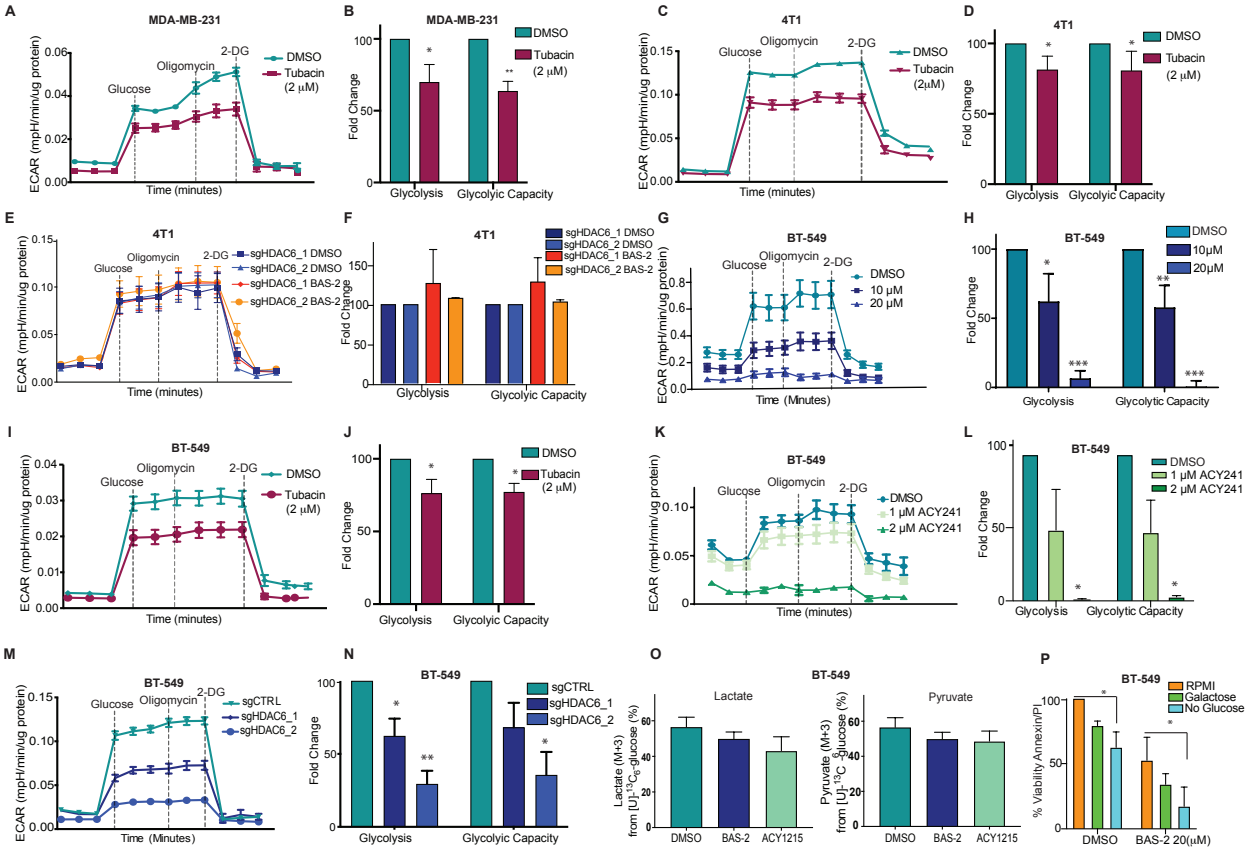

Fig. S5. The effect of inhibition and knockout of HDAC6 on metabolic pathways in TNBC. (**A**) ECAR traces (mpH/min/μg protein) for MDA231 cells treated with DMSO or Tubacin (2 μM) for 24 hrs (**B**) Fold change in glycolysis and glycolytic capacity was graphed (n=3, mean ± SEM, unpaired Student T-test). (**C**) ECAR traces for 4T1 cells treated with DMSO or Tubacin (2 μM) for 24 hrs. (**D**) Fold change in glycolysis and glycolytic capacity was analyzed (n=3, mean ± SEM, unpaired Student T-test). (**E**) ECAR traces for 4T1 cells following HDAC6 KO with or without BAS-2 treatment for 24 hr. (**F**) Fold change in glycolysis and glycolytic capacity was graphed (n=3, mean ± SEM). (**G**) ECAR traces for BT-549 cells treated with DMSO or BAS-2 for 24 hrs. (**H**) Fold change in glycolysis and glycolytic capacity was graphed (n=3, mean ± SEM). (**I**) Representative ECAR traces for BT-549 cells treated with DMSO or Tubacin (2 μM) for 24 hrs. (**J**) Fold change in glycolysis and glycolytic capacity was graphed (n=3, mean ± SEM) (**K**) Representative ECAR traces for BT-549 cells treated with DMSO or ACY-241 for 24 hrs. (**L**) Fold change in glycolysis and glycolytic capacity (n=3, mean ± SEM). (**M**) ECAR traces for BT-549 cells following HDAC6 KO. (**N**) Fold change in glycolysis and glycolytic capacity was graphed (n=3, mean ± SEM). (**O**) BT-549 cells were traced with 10 mM U_{13} glucose following 10 μM BAS-2 treatment or 1 μM of ACY1215 for 24 hrs. Percentage of lactate and pyruvate (M+3) from glucose are shown (n=3, mean ± SEM). (**P**) The percentage survival of BT-549 cells after

exposure to BAS-2 in the conditions indicated for 24 hrs (n=3, mean ± SEM). (**Q)** The percentage survival of BT-549 HDAC6 KO following growth in low glucose for 48 hr.

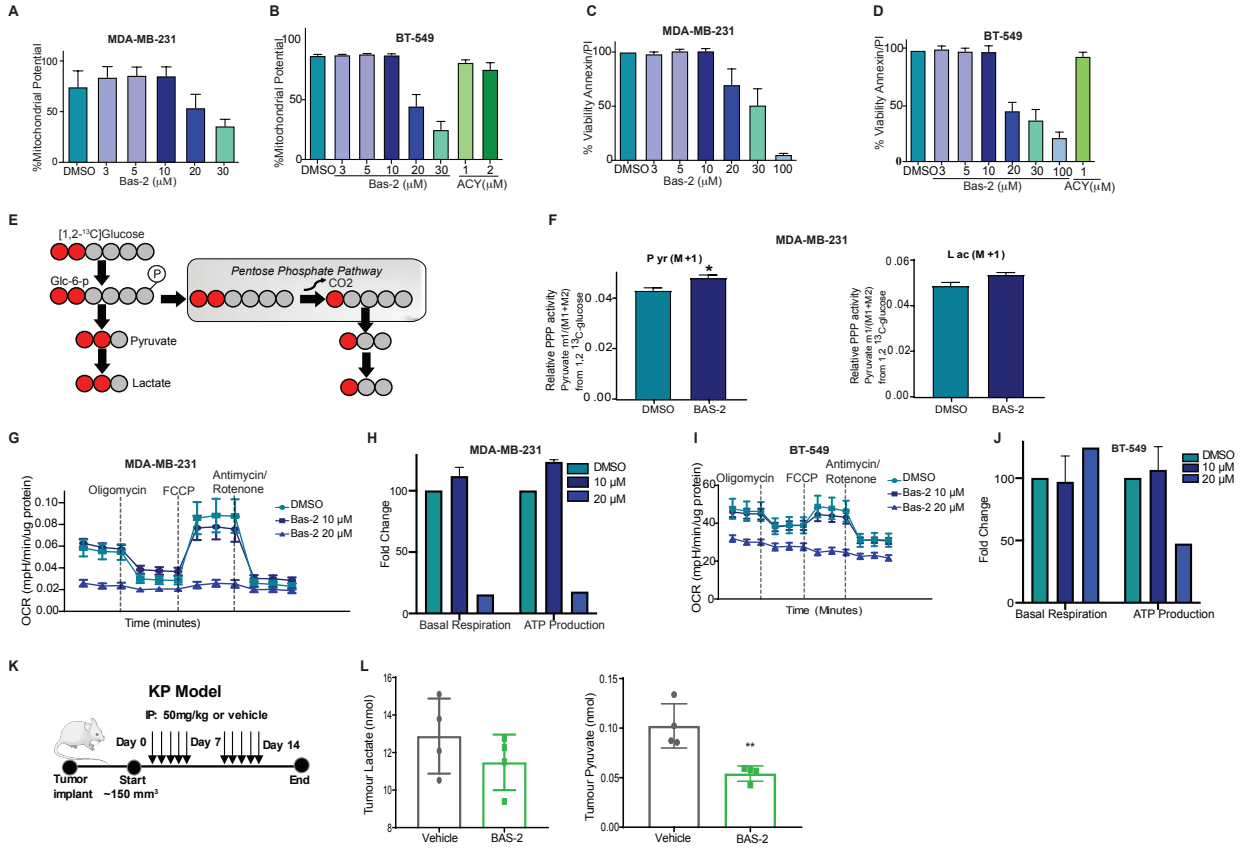

Fig. S6. The effect of inhibition of HDAC6 on metabolic pathways in TNBC and lung cancer models (**A** and **B**) Mitochondrial membrane potential in MDA231 cells (**A**) and BT-549 cells (**B**) following 24 hrs BAS-2 or ACY-241 treatment (n=3, mean ± SEM). (**C** and **D**) The percentage survival of MDA231 cells (**C**) and BT-549 cells (**D**) after exposure to BAS-2 or ACY-241 for 24 hrs (n=3, mean ± SEM). (**E**) MDA231 cells were traced with 10 mM 1,2-^{13}C glucose following 24 hrs with 10 μM BAS-2 treatment. (**F**) Percentage of lactate and pyruvate (M+1) from glucose are shown (mean ± SEM, n = 3). (**G**) OCR traces (mpH/min/μg protein) for MDA231 cells treated with BAS-2 (mean ± SEM). (**H**) Fold change in basal respiration and ATP production is plotted (n=3, mean ± SEM). (**I**) Same as (G) for BT-549 cells (**J**). Same as (H) for BT-549 cells. (**K**) C57BL/6 mice were subcutaneously inoculated with KP cells and following tumor formation mice were treated with vehicle or 50 mg/kg BAS-2. The mice were culled at day 14 (**L**) Metabolites were extracted from tumors and analyzed by GC-MS (n=4, mean ± SEM, unpaired Student T-test). (*P-value<0.05, ***P-value<0.001, 2-way ANOVA with Tukey post hoc test).

Data S1. (separate file)

Compounds used in the secondary cherry pick screen. Table provides information on the difference in response between the MDA231 siBAX/BAK cells and the MCF10a cells

Data S2. (separate file)

LCMS-MaxQuant analysis of proteins with increased acetylation in the presence of BAS-2 when compared to the DMSO control. Table provides information on the peptides which were altered in the presence of BAS2.

Data S3. (separate file)

LCMS-MaxQuant analysis of proteins with increased acetylation in HDAC6 KD cells. Table provides information on the peptides which were altered in the HDAC6 KD cells compared to control vector cells.

Data S4. (separate file)

List of proteins found to interact with immunoprecipitated HDAC6.